Genomic analyses unveil unprecedented human-induced demographic collapse and recovery in a wide-ranging cervid

Camille Kessler[1,3]*, Aaron B.A. Shafer[1,2]*

[1]Environmental and Life Sciences Graduate Program, Trent University, 7K9J 7B8 Peterborough, Ontario, Canada

[2]Department of Forensic Science, Trent University, 2140 East Bank Drive, Peterborough, ON K9J 7B8, Canada

[3]Lead contact

*Correspondence: camillekessler@trentu.ca (CK), aaronshafer@trentu.ca (ABAS)

Abstract

The glacial cycles of the Quaternary heavily impacted species through refugial contractions and post-glaciation expansions. Similarly, population demographic trajectories were intensely shaped by human pressures such as harvest and land use changes, particularly during the colonial-era. White-tailed and mule deer survived in different refugia during the last glacial maximum and were heavily impacted by the European colonisation as harvest and forestry practices drove white-tailed deer to extirpation in some regions, and severely reduced mule deer populations. Here, we analysed 73 re-sequenced deer genomes form across their North American range to understand the consequences of climatic and anthropogenic pressures on deer demographic history and adaptation. We found a strong signal of glacial-induced vicariance and demographic decline; notably, there is a severe decline in white-tailed deer effective population size (N_e) at the end of the Last Glacial Maximum. We found robust evidence for a colonial impact in the form of a recent and dramatic drop in N_e in all analysed populations, followed by a recovery in mainland white-tailed deer only. Historical census size and restocking data show a remarkable parallel to historical N_e estimates, while temporal N_e/N_c ratio shows patterns of conservation concern for mule deer. Signatures of selection highlight genes related to olfaction genes essential to deer biology and a cold receptor previously detected in woolly mammoth. We also detected numerous immune-genes that we surmise reflect the changing land-use patterns in North America. Our study provides a detailed picture of anthropogenic and climatic-induced decline in deer diversity, and clues to understanding the conservation concerns of mule deer and the incredible demographic recovery of white-tailed deer.

Keywords: Odocoileus, LGM, island population,

Introduction

Species abundance and distribution are impacted by both natural and anthropogenic factors. In the northern hemisphere, the glacial cycles of the Quaternary with the ice sheet advances, retreat, and corresponding sea level fluctuations[1–3], heavily impacted worldwide biota. These environmental changes dramatically affected demographic trajectories; cold periods forced species to adapt, move or retreat to refugia, their population decreasing or going extinct in the process, while warming episodes allowed for population expansion, colonisations[4], and adaptive divergence[5]. Several large mammals are hypothesised to have gone extinct primarily because of climate change during this period, notably the Eurasian musk ox (*Ovibos moschatus*), woolly rhinoceros (*Coelodonta antiquitatis*), and Steller's sea cow (*Hydrodamalis gigas*)[6–8].

The more recent Anthropocene also dramatically shaped demographic trajectories of wildlife through farming, harvest and logging[9,10]. Human pressures generally increased in the colonial era where settlers profoundly changed the land, leading to declines in endemic populations[11–16]. In Australia, for example, genomic analyses of seven extinct rodent species suggests a sudden demographic decline following the European colonisation[17]. The colonial impact has also been implicated in the extinction of the mainland Tasmanian devil (*Sarcophilus harrisii*) and blue antelope (*Hippotragus leucophaeus*)[18,19]. Beyond the demographic impacts, humans can also alter selection pressures experienced by populations through for example selective harvest, which could lead to artificial selection as has been suggested in brown bears (*Ursus arctos*), bighorn sheep (*Ovis canadensis*) and moose (*Alces alces*)[20–23].

Severe population contractions or bottlenecks increase genetic drift and risk of inbreeding, and can lead to the accumulation of mildly deleterious mutations[24,25], as seen in the woolly

mammoth and alpine ibex[26,27]. Additionally, population size fluctuations leave discernible genomic patterns along the genome: a declining population will exhibit a positive Tajima's D and a site frequency spectrum (SFS) that is relatively flat, whereas an expanding population will present a negative Tajima's D and a SFS skewed towards low-frequency alleles[28]. Depending on the extent of the contraction, both in magnitude and duration, such populations might also present with a low effective population size (N_e), particularly if the bottleneck was strong and the population took a while to recover[29]. In contrast, a population that remained steady over time, or one that recovered quickly from a bottleneck, will generally exhibit a larger N_e[25]. Genomic data can be used to model the changes in historical N_e[30–32], and recent analytical advancements allow for recent trends of N_e to be inferred[33]; collectively, this allows for disentangling historical climatic and modern anthropogenic factors shaping demographic history. Both contemporary and historical estimates of N_e when compared to census size appear to reflect adaptive potential and extinction risk[34,35].

The North American genus *Odocoileus* (deer) were heavily impacted by both the glacial cycles of the Pleistocene and European colonisation. Divergence estimates suggest the speciation between white-tailed (*O. virginianus*; WTD) and mule deer (*O. hemionus*; MD) took place between one and 3.13 Ma[36,37], with the group becoming among the most successful Cervids during glacial cycles[38]. White-tailed deer and MD are primarily found in North America, and both species survived in different refugia during the Last Glacial Maximum (LGM, 26 to 19 ka[39])[40–43]. Deer abundance is heavily monetised through hunting-related activities[44], and both species have been, and continue to be, important to indigenous communities as a source of food, clothing and culture[45,46]. White-tailed deer was likely the most abundant large-mammal prey in the late Holocene in eastern North America, and while some Indigenous People depended on

80 them for subsistence, indigenous harvest appeared to minimally impact WTD numbers[47,48]. In
81 contrast, European colonisation, specifically unregulated harvest and forestry practices,
82 resulted in heavily depleted and even extirpated WTD populations; this led to massive
83 restocking efforts across the United States in the 20th century[49]. Mule deer abundance is, and
84 was, lower than WTD, but MD populations were also diminished due to unregulated hunting,
85 hitting their low at the beginning of the 20th th century[50]. Stocking efforts were much less
86 pervasive in MD, and the species stabilized or recovered due to effective management
87 strategies[50–54].
88 Here, we aim to understand the consequences of climatic and anthropogenic pressures on
89 WTD & MD populations through demographic and selection analyses. We hypothesise that the
90 population genetic histories of North American deer were strongly impacted by the glacial
91 cycles of the Pleistocene and the European colonisation of the continent. We computed
92 genome-wide summary statistics, reconstructed WTD & MD demographic histories and
93 quantified genomic variation linked to environmental factors and selective forces.

94 *Materials and Methods*

95 Sampling & Sequencing

96 We sequenced the genomes of 73 deer collected across North America (Fig.1A, Table S1)
97 including published WGS data from 28 deer (PRJNA830519; Kessler et al., 2023). We extracted
98 DNA using the Qiagen DNeasy Blood and Tissue Kit following manufacturer's instructions and
99 checked concentration using Invitrogen Qubit assays. DNA was sent to The Centre for Applied
100 Genomics in Toronto, Canada, for library preparation and sequencing. All samples were
101 sequenced to an average of 4x coverage on an Illumina HiSeqX, except for four samples which
102 were re-sequenced to achieve higher coverage (> 15x; Table S1, Fig.1A).

103 We obtained census data for WTD and MD in the USA from 1450 to 2016[55], complemented up
104 to 2021 following the same methodology[56], and digitised restocking information for WTD in the
105 USA[49].

106 Data processing

107 We analysed and trimmed raw reads with FastQC (v0.11.9)[57] and Trimmomatic (v0.36)[58],
108 respectively. Using bwa-mem (v0.7.17)[59], we aligned raw reads to the WTD genome
109 (GCA_014726795.1) and sorted the reads using SAMtools sort (v1.10)[60]. We identified and
110 removed duplicates in Picard MarkDuplicates (v2.23.2)[61] and Sambamba view (v0.7.0)[62]. We
111 used GATK RealignerTargetCreator and IndelRealigner (v4.1.7.0)[63] to carry out a local re-
112 alignment and used Sambamba flagstat, mosdepth (v0.3.1)[64] and MultiQC (v1.10)[65] for quality
113 checks.

114 For sample sequenced on multiple lanes, we specified the read groups before removing
115 duplicates, and merged the sequencing files using Picard AddOrReplaceReadGroups and
116 MergeSamFiles, respectively. To have a consistent coverage among samples for non-SMC
117 demographic analyses, we down-sampled data to the average coverage of all other samples
118 (4x) using Picard DownsampleSam. We called the genotypes (-doGeno 4) and estimated
119 genotype likelihood using the GATK model (-gl 2) in ANGSD (v0.918)[66]. We retained SNPs with a
120 minimum base quality and a minimum mapQ quality of 20 (-minQ 20 & minMapQ 20) and a
121 minimum p-value of 1e-6 (-SNP_pval 1e-6).

122 Population subdivisions and summary statistics

123 We used PCAngsd (v1.02)[67] to investigate population clustering between and within species,
124 this program fits best our data as it is designed explicitly for low-coverage data and genotype
125 likelihoods. We investigated the relationship between the spread on the PCA and the

126 geographic distribution of our samples using a Pearson's correlation test in R (v4.2.0)[68]. We also
127 ran NGSadmix[69] to help decipher population structure in the MD samples. The program was
128 run with K = 1 up to K = 10 and 10 replicates, we identified the best K value using CLUMPAK [70,71].
129 We converted the hardcalls generated in ANGSD (.geno file) into a .vcf file using a Python script
130 (genoToVCF.py[72]) and retained only biallelic sites (--max-alleles 2) in VCFtools (v0.1.16)[73]. We
131 introduce the following convention to refer to populations supported by the PCAngsd and
132 NGSadmix and used in the following analyses (Fig.1B): mainland WTD = WTD_{ML}, Florida Keys
133 WTD = WTD_{KEY}, Mule deer subspecies = MD_{MD}, and MD black-tailed deer subspecies = MD_{BTD}.
134 Using VCFtools we computed weighted F_{st} between the four populations, as well as Tajima's D
135 and nucleotide diversity (π) per populations, all three processed in windows of 50kbp. We used
136 PLINK (v1.90b6.21)[74] to compute F_{ROH} on the 160 scaffolds representing the N90 of the WTD's
137 genome assembly, using the following non-default criteria: 100kb window size containing a
138 minimum of 50 SNPs, allowing up to three heterozygote sites and 10 missing calls per called
139 ROH. We computed F_{ROH} per individual using the sum of ROH sizes divided by the sum of N90
140 scaffolds length.

141 Demographic inference

142 We inferred the historical demography of WTD_{KEY}, WTD_{ML}, MD_{MD} and MD_{BTD} by implementing the
143 multiple sequentially Markovian coalescent (MSMC) model[31] that generates estimates of N_e
144 over time. Here we used four high-coverage samples from both WTD population and MD
145 subspecies (Fig.1A, Table S1). We first generated a 35-mer mappability mask file using SNPable
146 as is required for MSMC with more than one sample[32]. We also phased the samples with
147 whathap (v1.3)[75] and filtered out scaffolds shorter than 500 Kbp. We ran MSMC2, including 100
148 bootstraps, using 1×2+25×1+1×2+1×3 as time segment pattern. To estimate the cross-

149 coalescence rate across populations, we carried out a pairwise comparison of the first
150 haplotype from each sample using the -P flag and skipped any sites with ambiguous phasing.
151 To test and account for ancestral migration, we implemented MSMC-IM[76], assuming a
152 generation time of 2 years[77,78] and a mutation rate of 1.33x10-8 mutations/site/generation.
153 We then used GONE[33] to compute demographic history in the recent past from patterns of
154 linkage disequilibrium for the four populations (WTD_{KEY}, WTD_{ML}, MD_{MD} and MD_{BTD}). We restricted
155 this analysis to the 160 scaffolds representing the N90 of the WTD assembly, input map files
156 were produced from vcf in PLINK. We ran GONE with 500 repetitions on 500 generations with
157 30,000 SNPs per chromosome, a minor allele frequency pruning of 0.01, a hc value of 0.04, a
158 recombination rate of 0.5 for WTD populations and 0.35 for the MD populations [36]. We
159 compared the census size (N_c) estimate from Webb[55] to the N_e resulting from GONE to obtain a
160 contemporary N_e/N_c ratio over time.
161 To model explicitly the demographic history of WTD and MD, we further filtered the dataset in
162 VCFtools to I) account for linkage disequilibrium by removing sites that were within 10kbp of
163 each other (--thin 10000), and II) remove all missing data (--max-missing 1). To compute the
164 folded site frequency spectrum, we used δaδi (v 2.1.1)[79] and dadi_pipeline (v3.1.7)[80] with default
165 settings and four repetitions to optimise and fit demographic models. We performed two
166 different demographic comparisons: 1) WTD_{KEY}, WTD_{ML} and all MD, and 2) MD_{MD}, MD_{BTD} and
167 WTD_{ML} as outgroup. We selected relevant models involving migration and asynchronous
168 splitting (Table S2), and the best model was selected based on the log-likelihood and its
169 consistency across runs. The best model was additionally run with 100 bootstrapped
170 frequency spectrums to quantify uncertainty. We used the N_c estimates taken from Webb[55,56] to

171 the ancestral N_e taken from NuA values in the δaδi analysis to obtain ancestral N_e/N_c ratio over
172 time for both species.

173 Adaptive divergence

174 We used a redundancy analysis (RDA) to detect genotype-environment association and loci
175 under local adaptation across individuals. We collected 19 bioclimatic variables at a resolution
176 of 2.5' from WorldClim2 using the R package raster (v.3.6-3)[81,82] and extracted the values
177 corresponding to the coordinates of our samples. As RDA analyses are problematic when using
178 highly correlated variables, we investigated the Pearson correlation between the 19
179 bioclimatic variables, latitude, longitude and removed predictors that showed a correlation
180 higher than 0.7[83]. For the dataset comprising all individuals, we additionally included a variable
181 for the species. We carried out the analyses with the R package vegan (v.2.6-4)[84] based on the
182 datasets created for demographic modelling. We investigated conditional models with the
183 condition set as either the bioclimatic variables or the longitude.

184 We computed the integrated haplotype score (iHS) and the extended haplotype homozygosity
185 (EHH) on the scaffolds representing the N90 of the WTD reference genome to detect regions
186 under selection in the four populations. We started by phasing our data in SHAPEIT (v2.r904[85]),
187 then calculated and normalised the selection statistics in vcflib (v1.0.3[86]) with the functions iHS
188 and normalize-iHS and default settings. We identified peaks in the most extreme 1% iHS values
189 in R using the function findPeaks[87] and extracted the gene IDs in 50Kbp windows. The genes
190 with available entry IDs were uploaded to Uniprot[88] for ID mapping where we retrieved the gene
191 names and functions. The list was manually curated, and each gene was assigned to one or
192 more of the following categories based on its function: reproduction, immunity, physiology,
193 metabolism, sensory perception, development, and other.

194 We analysed all results and produced all the graphics in R.

195 ## *Results*

196 ### Population subdivisions and summary statistics

197 We called 144,634,190 SNPs from 73 individuals at a coverage of 4x on average. The PCA on
198 allele frequencies of all individuals presents a clear species delimitation along PC1 which
199 explained 46% of the variation, whereas PC2 separated the WTD_{KEY} individuals (Fig.1B). WTD-
200 specific PCAs showed the delimitation between WTD_{ML} and WTD_{KEY} individuals (PC1); PC2
201 strongly correlated with longitude (Pearson correlation = -0.88, p-value = < 2.2e-16) and
202 accounted for 7% of the variation (Fig.S1A). In the MD PCA, PC1 correlated to longitude
203 (Pearson correlation = 0.83, p-value = 5.96e-06), with PC2 associated to latitude (Pearson
204 correlation = 0.47, p-value = 0.037, Fig.S1B). The MD PCA showed one clear cluster of 13
205 samples; we clarified the population identity of the seven remaining individuals using
206 NGSadmix that assigned two admixed individuals to the first cluster (MD_{MD})and identified a
207 second population of five individuals (MD_{BTD}; Fig.S1C).

208 Weighted F_{st} measures are very high between species (0.36 - 0.58); intra-specific comparisons
209 ranged from 0.12 to 0.17 (Table S3). Tajima's D values were positive only for the WTD_{KEY}
210 population (0.11), all three other exhibited negative values, the lowest being -0.89 for WTD_{ML}
211 (Table 1). F_{ROH} values were lowest in the MD populations (<= 0.3%), where WTD_{KEY} presented the
212 highest F_{ROH} value (1.4%; Table 1)

213 ### Demographic inference

214 We inferred the demography of four high-coverage samples, one per population, using MSMC2
215 analysis. The trajectories of the four samples split at approximately 600 ka where the MD_{MD}
216 population start declining whereas WTD populations keep increasing (Fig.2A). Both MD

217 population trajectories are very similar and show a general steady decline. WTD_{KEY} appear to
218 decline about 46 ka, whereas WTD_{ML} drastically increased to peak at an N_e of >1 million
219 individuals, followed by a clear crash at the end of the LGM (Fig.2A). Species split times inferred
220 by the cross-coalescence rate of the MSMC-IM model is about 500 ka (Fig.S2A), the within-
221 species split times are estimated at approximately 25 ka between WTD_{ML} and WTD_{KEY}, and
222 about 70 ka for MD_{MD} and MD_{BTD}(Fig.S2B).
223 The N_e of WTD_{KEY} appears very low and stable for the last ~400 years, reaching its lowest at ~350
224 individuals (Fig.2B). Temporally, the WTD_{ML} population decreased with variable intensity that
225 ended with a drastic decline to a N_e of ~2000 between 126- and 142-years BP. Following this
226 severe drop, the WTD_{ML} population rapidly rebounded to reach a current effective population
227 size estimated at just under 5M individuals (Fig.2B); this clearly correlates with census data and
228 restocking efforts (Fig.2C). Both MD populations exhibited a slow but steady increase until
229 approximately 300 years ago, after which both trajectories show a gradual decline ending with
230 a severe drop without recovery (Fig.2B). MD N_e patterns are more decoupled from the census
231 data; N_c here shows a crash in both MD_{MD} and MD_{BTD} with N_e lagging. A subsequent small
232 recovery of MD_{MD} N_e is visible (Fig.2C), but the contemporary N_e/N_c ratio is higher and more
233 variable for MD (mean = 0.49, var = 0.3 vs WTD mean = 0.18 & var = 0.01) with values from the
234 last century mostly below 0.1. Both species have a lower ancestral N_e/N_c ratio with low
235 variability, the averages are of 0.06 and 0.01 for WTD and MD, respectively. WTD's historical
236 ratio (var = 0.03) is more variable than MD's (var = 0.0001) and the contemporary WTD (Fig.3).
237 Finally, we modelled the demographic history of our four populations using the site frequency
238 spectra. For our first comparison, we analysed the demographic history of the trio WTD_{KEY} –
239 WTD_{ML} – MD, the best model supports adjacent secondary contact between populations (Fig.

240 4A). This model shows a general MD decline, and a WTD expansion followed by a decline,
241 including secondary contact between adjacent populations (Fig.4A, table 2). Notably, there
242 was a demographic crash in WTD_{KEY} at approximately 6 ka. In our second trio, we investigated
243 the relationship between MD_{MD} – MD_{BTD} – WTD_{ML} for which the best model suggests a secondary
244 contact between WTD_{ML} – MD_{MD} that predates the split between the two MD populations.
245 Ancient migration between WTD_{ML} and MD is extremely low, but migration increases over time;
246 this model also suggests population expansion for WTD_{ML} but a decline for both MD_{BTD} and
247 MD_{MD} (Fig.4B, table 2).

248 Adaptive divergence

249 We conducted three redundancy analyses to identify genotypes linked to environmental
250 variables and loci under local adaptation. The full model inter-specific RDA explained 16.5% of
251 the variation, but most of the variation was driven by the species variable (Table 3, Fig.S5A).
252 The full model for the WTD explained 6.32% of the variation and included five predictors - BIO1,
253 BIO2 (mean diurnal range), BIO8 (mean temperature of wettest quarter), BIO15 (precipitation
254 seasonality) and longitude being significant (Table 3, Fig.S5B). There were 12,206 outlier SNPs
255 predominantly associated with annual mean temperature (BIO1; Table 3, Fig.S5C). In the
256 redundancy analysis on MD individuals, we found only BIO2 and BIO16 (precipitation of wettest
257 quarter) were significant predictors, and found 7434 outlier SNPs, most of which were
258 associated with the variable BIO16 (Table 3).

259 We found a total of 443 genes within 25 Kbp of an iHS peaks, including 249 with an existing
260 Entry ID and identified function (Table S4). There were 121 genes around iHS peaks in the
261 WTD_{ML} population, 45 of which we could assign an explicit category. Most were assigned to
262 immunity (18 genes), including two genes related to the major histocompatibility complex

263 (MHC): *HLA-DQA1* and *HLA-DQB*. Additionally, we found two genes linked to sensory perception:
264 one odorant receptor (*OR5D18*) and one cold receptor (TRPM8, Table S4). We identified 23
265 genes surrounding iHS peaks in the WTD_{KEY}, including one MHC gene: *HLA-DRB4*. For the MD_{MD}
266 population, we could explicitly categorise 34 genes on a total of 95 neighbouring iHS peaks.
267 They include four MHC genes: *HLA-DQA1*, *HLA-DQB1*, *HLA-DRB3* and *HLA-DRB4,* another gene
268 related to the MHC: *HIVEP2*, three genes described as olfactory or odorant receptors (*OR51I1*,
269 *OR5D18*, *TAAR5*), and one cold receptor (*GRIK2*). Finally, we identified 26 genes adjacent to iHS
270 peaks in the MD_{BTD} population.

Discussion

Both climatic and anthropogenic impact have had roles in the demographic trajectories of species around the globe[7–9].The complex climatic cycles of the Pleistocene, concluding with the LGM, generally forced species to move from a wide range into smaller, often isolated refugia[4]. Subsequently, the peopling of North America[89] and the colonisation by Europeans several millennia later represented further pressures to many populations inhabiting the continent[13,49,90]. Here, we reconstructed the demographic history and signals of selection of white-tailed and mule deer to improve our understanding of climatic and anthropogenic pressures on these enigmatic North American species. Through extensive genomic analysis we observed a remarkable overlap between climate and human drivers and WTD N_e, and provide the first temporal N_e/N_c assessment based on whole genome sequencing, with contemporary evaluations of MD supporting the demographic concerns facing this species[51,55].

Strong climatic impact on deer populations

The glacial cycles of the Quaternary forced populations to move or adapt, resulting in population divergence[91,92], decline[93–96] and even replacement[97]. Consistently, our results show the clear impact of climate on WTD during the late Quaternary: while WTD populations did not appear to be heavily impacted by glacial cycles prior to ~250 ka, the period starting ~190 ka onwards shows large changes in N_e that mirror climatic fluctuations (Fig.2A). A striking example is WTD_{ML} for which we observe an intense N_e drop the coincides with the LGM. WTD populations were may have been separated into different refugia during this period[37,41,98,99] with a collective contraction that left a strong signal on the WTD genome. Similarly, the Key deer (*O. v. clavium*), considered a subspecies of WTD, showed a constant decline that predated the LGM, with a clear separation from WTD_{ML} ~20 ka (Fig.2A; S2A). Key deer were thought to have become

294 permanently isolated ~8,000 ka[41,100]; which is reflected by the demographic decline recovered
295 in the δaδi analysis around this time (Table 2). This separation and isolation led to a clear loss
296 of genomic diversity and accumulation of deleterious alleles in the Florida keys[101], and they are
297 currently listed as Endangered[102]. The collective demographic methods here accurately
298 pinpoint the LGM as a driver of subdivision and declines in WTD.
299 The LGM is implicated in the MD_{MD} and MD_{BTD} separation, where subspecies were separated in
300 different refugia which increased intra-specific divergence[37,40,43]. Our results are somewhat
301 equivocal as our CCR estimate a MD/BTD split approximately 70 ka but δaδi places it closer to
302 the LGM. Pre-split, the common ancestor of MD_{MD} and MD_{BTD} appeared lower, but stable
303 through time, in stark contrast to the WTD populations (Fig.2A). As MD are prone to population
304 fluctuations[103], and N_e is most strongly influenced by long periods of low N_c[104], the overall stable
305 historical N_e is consistent with population genetic theory. Cold adaptation might also have
306 been the determinant factor in this stability as MD are the most tolerant to cold climates[105].
307 Interestingly, we found selection patterns at the genes *GRIK2* in MD_{MD} and *TRPM8* in WTD_{ML}, both
308 conferring sensitivity to cold temperature (Table S4). Mutations identified in woolly
309 mammoth's *TRPM8* were suggested to be linked to the species' adaptation to cold climates[106].
310 **Human-induced collapse, varying selection pressures on white-tailed deer**
311 Driven by overharvest and change in land use for agriculture and logging, historical decline and
312 near extirpation of WTD has been thoroughly documented in the USA[49]. The timing differed
313 depending on the region, with for example Illinois WTD reaching their lowest population size
314 in 1878 and Montana in 1941[49]. This depletion led managers to supplement deer populations
315 with translocations[49] (Fig.2C). The WTD_{ML} population quickly rebounded, and analyses of the
316 nearly extirpated populations of Mississippi and Missouri show that the bottleneck had little to

317 no effect on deer's genetic variation[78,107]. The apparent absence of diversity consequences from
318 a bottleneck has also been observed in the deer introductions on Anticosti Island (Québec,
319 Canada) where WTD retained a high genetic diversity[108], and on St. John (Virgin Islands, USA)
320 where deer show high heterozygosity and low inbreeding[109]. Despite this apparent high
321 diversity, which we also see across the genome (Table 1), a detailed assessment of deleterious
322 alleles showed a high genetic load for WTD[101,110], with a putative link to stocking efforts[110].
323 Purging does not appear to have taken place in WTD[110], which might be cause for concern for
324 isolated populations with high loads like the Florida Keys[101].
325 The fluctuations in historical census sizes combined with the restocking data depict a clear
326 history of WTD decline and recovery in the USA (Fig.2C). The recent demographic trajectory of
327 the WTD_{ML} population strikingly mirrors census size estimates (Fig.2B); this presented us with a
328 unique opportunity to measure N_e/N_c over time which showed a stable relationship in WTD
329 (Fig.3). The high adaptive potential of WTD combined with the recent demographic collapse
330 (species wide lowest N_e ~1800) and recovery, allows us to suggest that any detected sweep that
331 is not fixed is likely the result of selection in the past 150 years. In mainland WTD, we found a
332 wide variety of immunity-related genes, including two MHC genes potentially under selection
333 which would suggest selection pressures from pathogens (Table S4). WTD are subject to many
334 diseases, some of which have arisen recently from livestock, such as the epizootic
335 haemorrhagic and chronic wasting disease, as well as a variety of tick-borne diseases[111]. WTD
336 is also the main reservoir of bovine tuberculosis on the continent with strong repercussions in
337 cases of transmission to cattle[111]. While immune genes often are detected in genome scans,
338 their presence in WTD scans is consistent with the large land use changes that have transpired
339 in North America over the past two centuries.

340 Previous analyses suggest that some olfactory genes are under balancing selection in deer[36],
341 we detected this function here again with the gene *OR5D18* under positive selection. In WTD,
342 smell is critical for predator response, sociality, and foraging, however little is known about the
343 genetics of this essential sense. We also found seven genes involved in fertilisation,
344 spermatogenesis, or sperm morphology (Table S5). As WTD & MD hybridise in areas of
345 sympatry[37,98,112] and as previous analyses suggest hybrid incompatibilities[36], we highlight the
346 potential of those genes in this context. Particularly, the gene RFX2 which is necessary for
347 spermatogenesis in mice[113], and *ASTL* and *RABL2A* that are linked to infertility[114,115].

348 **Delayed collapse but similar selection pressures on mule deer**

349 Human Settlements on the MD historic range were estimated at less than 20 in 1800, and while
350 harvest likely depressed populations in the surrounding areas, the rest of the range probably
351 saw minimal impact[50]. Over time and with the increased settlements in western North America,
352 MD populations strongly declined from the end of the 19th century throughout the range[50]. In
353 Colorado for example, while MD were deemed abundant in the 19th century only to become
354 rare between 1900 and 1930[51,53]. This is consistent with our analysis which shows a sharp
355 decrease in the MD_{MD} population during that period, though the MD_{BTD} population decline
356 appeared later. These population reductions also appeared to happen after the WTD collapse,
357 possibly reflecting the later western wave of settlers and more recent land use changes; as a
358 migrating species MD might respond more to human-induced habitat change. For example,
359 the limitation in winter range habitat appears to be driving MD decline in Colorado[51,53]. Thus,
360 collectively the delayed and decoupling of N_e from N_c, and more muted temporal response of
361 N_e, is consistent the species ecology and human intervention history.

362 In MD_{MD}, we found many immunity-related genes under selection, including one MHC gene
363 unique to this population (*HLA-DRB3*, Table S4). Diseases affecting MD are often the same that
364 infect WTD, including the risk of spilling over to and from livestock[111]. Chronic wasting disease
365 is of particular concern for this MD: it is considered as a major factor in the species decline in
366 many regions[116], with the genomic and immune response clearly polygenic[117]. Regarding
367 sensory perception and in addition to the cold receptor *GRIK2*, we identified two odorant
368 receptors and two trace amine receptors as potentially under selection in this population,
369 olfaction is just as critical for MD as it is for WTD. Finally, linked to reproduction, we find *RFX2*
370 as in WTD_{ML}, as well as two other genes unique to this population and involved in sperm
371 morphology or differentiation (Table S4).

372 **Variable N_e/N_c ratio through time**

373 The N_e/N_c ratio is informative on the genomic health and demographic histories of species,
374 which is why it has often been used to assess populations of management and conservation
375 concern[35,118,119]. Indeed, a population exhibiting a low contemporary N_e/N_c ratio is more subject
376 to rapid loss in genetic diversity than populations with a higher ratio[35,118]. While, this ratio is
377 highly variable between taxa, the generally accepted median of concern in wild populations is
378 0.1[118,120]. The seven most recent values for MD are all below 0.1 and overall, the more recent
379 time points show higher variability in contemporary N_e/N_c (Fig.3). The larger fluctuations in
380 MD's N_c in the last 100 years have led to a decoupling of N_e and N_c and reflect the species higher
381 demographic stochasticity. This recent reduced ratio could mean that the species is at risk of
382 faster loss of genetic diversity and echoes other calls of concern[51,53]. Interestingly, historical
383 N_e/N_c ratio presents low variability for both species and no immediate red flag[34]; this ratio is

clearly driven by the high N_c of both species, and focused sampling of isolated populations might reveal a different pattern as seen in caribou[121].

Conclusion

The dramatic drop in N_e in the recent past of all deer populations studied here is robust evidence for a colonial impact through unregulated hunting and changes in land use. Even though WTD & MD populations were heavily depleted, both species showed signs recovery, particularly white-tailed deer, from restocking efforts. While diversity and demographic trends appear positive, there is also a high genetic load in WTD[110], and a low contemporary N_e/N_c ratio in MD. Selection surrounding a wide variety of genes, including some of biological importance in WTD & MD such as genes related to immunity, olfaction, and reproduction appear evident. Historical sampling of *Odocoileus* will prove informative for disentangling human-induced selection and genetic load in these wide-ranging cervids.

Acknowledgements

Camille Kessler was supported by an International Graduate Scholarship. This work was supported by NSERC Discovery Grant (Grant Number: RGPIN-2017- 03934); ComputeCanada Resources for Research Groups (Grant Number: RRG gme-665-ab); Canadian Foundation for Innovation: John R. Evans Leaders Fund and the Ontario Early Researcher Award (Grant Number: #36905). For providing samples, we thank Alan Cain, Steeve Côté, Anh Dao, Marco Festa-Bianchet, Brad Fulk, Eric Hoffman, Levi Jaster, Daniel Koelsch, Emily Latch, Brent Patterson, Joe Nocera, Don Stewart & Russell Easy, Jonathan Shaw, David Walter and Jon Wheeler. We also thank Jose Alberto López Alemán for commenting on the text.

We sampled deer from across North America, a stolen land which remains a home to many First Peoples and Trent University is located on the traditional territory of the Michi Saagiig

Anishnaabeg. As settlers, we are grateful to have had the opportunity to live and work on this land, and to benefit from it. We would like to show our respect to the First Peoples and thank them for their care, stewardship, and teachings. Miigwetch.

Data Accessibility

Raw reads for the 45 deer additional individuals were deposited on the NCBI Sequence Read Archive (Accession number PRJNA830519). All scripts are available on GitLab (https://gitlab.com/WiDGeT_TrentU/graduate_theses/-/tree/master/Kessler/CH_02).

Author contributions

CK and ABAS conceived the study, ABAS collected the samples, CK performed the molecular laboratory work and the bioinformatic analyses with contribution from ABAS for MSMC2, CK and ABAS wrote the manuscript.

Declaration of interests

CK and ABAS declare no competing interests.

References

1. Allen, J.R.M., Forrest, M., Hickler, T., Singarayer, J.S., Valdes, P.J., and Huntley, B. (2020). Global vegetation patterns of the past 140,000 years. J Biogeogr *47*, 2073–2090. 10.1111/jbi.13930.

2. Batchelor, C.L., Margold, M., Krapp, M., Murton, D.K., Dalton, A.S., Gibbard, P.L., Stokes, C.R., Murton, J.B., and Manica, A. (2019). The configuration of Northern Hemisphere ice sheets through the Quaternary. Nat Commun *10*, 3713. 10.1038/s41467-019-11601-2.

3. Gowan, E.J., Zhang, X., Khosravi, S., Rovere, A., Stocchi, P., Hughes, A.L.C., Gyllencreutz, R., Mangerud, J., Svendsen, J.-I., and Lohmann, G. (2021). A new global ice sheet reconstruction for the past 80 000 years. Nat Commun *12*, 1199. 10.1038/s41467-021-21469-w.

4. Shafer, A.B.A., Cullingham, C.I., Côté, S.D., and Coltman, D.W. (2010). Of Glaciers and Refugia: a Decade of Study Sheds New Light on the Phylogeography of Northwestern North America. Molecular Ecology *19*, 4589–4621. 10.1111/j.1365-294X.2010.04828.x.

5. Pamilo, P., and Savolainen, O. (2004). Post-Glacial Colonization, Drift, Local Selection and Conservation Value of Populations: A Northern Perspective. Hereditas *130*, 229–238. 10.1111/j.1601-5223.1999.00229.x.

6. Lord, E., Dussex, N., Kierczak, M., Díez-del-Molino, D., Ryder, O.A., Stanton, D.W.G., Gilbert, M.T.P., Sánchez-Barreiro, F., Zhang, G., Sinding, M.-H.S., et al. (2020). Pre-extinction Demographic Stability and Genomic Signatures of Adaptation in the Woolly Rhinoceros. Current Biology *30*, 3871-3879.e7. 10.1016/j.cub.2020.07.046.

7. Lorenzen, E.D., Nogués-Bravo, D., Orlando, L., Weinstock, J., Binladen, J., Marske, K.A., Ugan, A., Borregaard, M.K., Gilbert, M.T.P., Nielsen, R., et al. (2011). Species-specific responses of Late Quaternary megafauna to climate and humans. Nature *479*, 359–364. 10.1038/nature10574.

8. Sharko, F.S., Boulygina, E.S., Tsygankova, S.V., Slobodova, N.V., Alekseev, D.A., Krasivskaya, A.A., Rastorguev, S.M., Tikhonov, A.N., and Nedoluzhko, A.V. (2021). Steller's sea cow genome suggests this species began going extinct before the arrival of Paleolithic humans. Nat Commun *12*, 2215. 10.1038/s41467-021-22567-5.

9. Ceballos, G., Ehrlich, P.R., Barnosky, A.D., García, A., Pringle, R.M., and Palmer, T.M. (2015). Accelerated modern human–induced species losses: Entering the sixth mass extinction. Sci. Adv. *1*, e1400253. 10.1126/sciadv.1400253.

10. IPCC (2022). Climate change 2022: Impacts, adaptation and vulnerability. 3–33.

11. Peros, M.C., Munoz, S.E., Gajewski, K., and Viau, A.E. (2010). Prehistoric demography of North America inferred from radiocarbon data. Journal of Archaeological Science *37*, 656–664. 10.1016/j.jas.2009.10.029.

12. Tavares, G.M., Reales, G., Bortolini, M.C., and Fagundes, N.J.R. (2019). Measuring the impact of European colonization on Native American populations in Southern Brazil and Uruguay: Evidence from mtDNA. Am J Hum Biol *31*, e23243. 10.1002/ajhb.23243.

13. Lindo, J., Huerta-Sánchez, E., Nakagome, S., Rasmussen, M., Petzelt, B., Mitchell, J., Cybulski, J.S., Willerslev, E., DeGiorgio, M., and Malhi, R.S. (2016). A time transect of exomes from a Native American population before and after European contact. Nat Commun *7*, 13175. 10.1038/ncomms13175.

14. Stevens, N., Bond, W., Feurdean, A., and Lehmann, C.E.R. (2022). Grassy Ecosystems in the Anthropocene. Annu. Rev. Environ. Resour. *47*, 261–289. 10.1146/annurev-environ-112420-015211.

15. Brain, R.A., and Prosser, R.S. (2022). Human induced fish declines in North America, how do agricultural pesticides compare to other drivers? Environ Sci Pollut Res *29*, 66010–66040. 10.1007/s11356-022-22102-z.

16. Woinarski, J.C.Z., Burbidge, A.A., and Harrison, P.L. (2015). Ongoing unraveling of a continental fauna: Decline and extinction of Australian mammals since European settlement. Proc. Natl. Acad. Sci. U.S.A. *112*, 4531–4540. 10.1073/pnas.1417301112.

17. Roycroft, E., MacDonald, A.J., Moritz, C., Moussalli, A., Portela Miguez, R., and Rowe, K.C. (2021). Museum genomics reveals the rapid decline and extinction of Australian rodents since European settlement. Proc Natl Acad Sci USA *118*, e2021390118. 10.1073/pnas.2021390118.

18. Brüniche–Olsen, A., Jones, M.E., Burridge, C.P., Murchison, E.P., Holland, B.R., and Austin, J.J. (2018). Ancient DNA tracks the mainland extinction and island survival of the Tasmanian devil. J Biogeogr *45*, 963–976. 10.1111/jbi.13214.

19. Hempel, E., Bibi, F., Faith, J.T., Koepfli, K.-P., Klittich, A.M., Duchêne, D.A., Brink, J.S., Kalthoff, D.C., Dalén, L., Hofreiter, M., et al. (2022). Blue Turns to Gray: Paleogenomic Insights into the Evolutionary History and Extinction of the Blue Antelope (Hippotragus leucophaeus). Molecular Biology and Evolution *39*, msac241. 10.1093/molbev/msac241.

20. Allendorf, F.W., and Hard, J.J. (2009). Human-induced evolution caused by unnatural selection through harvest of wild animals. Proc. Natl. Acad. Sci. U.S.A. *106*, 9987–9994. 10.1073/pnas.0901069106.

21. Coltman, D.W., O'Donoghue, P., Jorgenson, J.T., Hogg, J.T., Strobeck, C., and Festa-Bianchet, M. (2003). Undesirable evolutionary consequences of trophy hunting. Nature *426*, 655–658. 10.1038/nature02177.

22. Kvalnes, T., Saether, B.-E., Haanes, H., Røed, K.H., Engen, S., and Solberg, E.J. (2016). Harvest-induced phenotypic selection in an island population of moose, Alces alces. Evolution *70*, 1486–1500. 10.1111/evo.12952.

23. Van De Walle, J., Pigeon, G., Zedrosser, A., Swenson, J.E., and Pelletier, F. (2018). Hunting regulation favors slow life histories in a large carnivore. Nat Commun *9*, 1100. 10.1038/s41467-018-03506-3.

24. Frankham, R. (2005). Genetics and extinction. Biological Conservation *126*, 131–140. 10.1016/j.biocon.2005.05.002.

25. Charlesworth, B. (2009). Effective population size and patterns of molecular evolution and variation. g e n e ti c s, 11.

26. Palkopoulou, E., Mallick, S., Skoglund, P., Enk, J., Rohland, N., Li, H., Omrak, A., Vartanyan, S., Poinar, H., Götherström, A., et al. (2015). Complete Genomes Reveal Signatures of Demographic and Genetic Declines in the Woolly Mammoth. Current Biology *25*, 1395–1400. 10.1016/j.cub.2015.04.007.

27. Grossen, C., Guillaume, F., Keller, L.F., and Croll, D. (2020). Purging of highly deleterious mutations through severe bottlenecks in Alpine ibex. Nat Commun *11*, 1001. 10.1038/s41467-020-14803-1.

28. Hahn, M.W. (2018). Molecular population genetics (Oxford University Press; Sinauer Associates).

29. Martchenko, D., and Shafer, A. (2022). Contrasting whole-genome and reduced representation sequencing for population demographic inference: an alpine mammal example. 10.22541/au.164190604.45542461/v1.

30. Li, H., and Durbin, R. (2011). Inference of human population history from individual whole-genome sequences. Nature *475*, 493–496. 10.1038/nature10231.

31. Schiffels, S., and Durbin, R. (2014). Inferring Human Population Size and Separation History from Multiple Genome Sequences. Nat Genet *46*, 919–925. 10.1038/ng.3015.

32. Schiffels, S., and Wang, K. (2020). MSMC and MSMC2: The Multiple Sequentially Markovian Coalescent. In Statistical Population Genomics Methods in Molecular Biology., J. Y. Dutheil, ed. (Springer US), pp. 147–166. 10.1007/978-1-0716-0199-0_7.

33. Santiago, E., Novo, I., Pardiñas, A.F., Saura, M., Wang, J., and Caballero, A. (2020). Recent Demographic History Inferred by High-Resolution Analysis of Linkage Disequilibrium. Molecular Biology and Evolution *37*, 3642–3653. 10.1093/molbev/msaa169.

34. Wilder, A.P., Supple, M.A., Subramanian, A., Mudide, A., Swofford, R., Serres-Armero, A., Steiner, C., Koepfli, K.-P., Genereux, D.P., Karlsson, E.K., et al. (2023). The contribution of historical processes to contemporary extinction risk in placental mammals. Science *380*, eabn5856. 10.1126/science.abn5856.

35. Palstra, F.P., and Ruzzante, D.E. (2008). Genetic estimates of contemporary effective population size: what can they tell us about the importance of genetic stochasticity for wild

population persistence? Molecular Ecology *17*, 3428–3447. 10.1111/j.1365-294X.2008.03842.x.

36. Kessler, C., Wootton, E., and Shafer, A.B.A. (2023). Speciation without gene-flow in hybridizing deer. Molecular Ecology *32*, 1117–1132. 10.1111/mec.16824.

37. Wright, E.A., Roberts, E.K., Platt, R.N., Bayouth, J.V., Conway, W.C., and Bradley, R.D. (2022). Mitochondrial capture and subsequent genetic divergence generates a novel haplogroup: evidence from ancient and ongoing hybridization in mule and white-tailed deer. Journal of Mammalogy *103*, 723–736. 10.1093/jmammal/gyab156.

38. Hewitt, D.G. (2011). Biology and management of white-tailed deer (CRC Press).

39. Clark, P.U., Dyke, A.S., Shakun, J.D., Carlson, A.E., Clark, J., Wohlfarth, B., Mitrovica, J.X., Hostetler, S.W., and McCabe, A.M. (2009). The Last Glacial Maximum. Science *325*, 710–714. 10.1126/science.1172873.

40. Latch, E.K., Heffelfinger, J.R., Fike, J.A., and RHODES Jr, O.E. (2009). Species-wide Phylogeography of North American Mule Deer (Odocoileus hemionus): Cryptic Glacial Refugia and Postglacial Recolonization. Molecular Ecology *18*, 1730–1745. 10.1111/j.1365-294X.2009.04153.x.

41. Ellsworth, D.L., Honeycutt, R.L., Silvy, N.J., Bickham, J.W., and Klimstra, W.D. (1994). Historical Biogeography and Contemporary Patterns Of Mitochondrial DNA Variation In White-Tailed Deer From The Southeastern United States. Evolution *48*, 122–136. 10.1111/j.1558-5646.1994.tb01299.x.

42. Greenslade, A.D. (1998). Inter- and intraspecific phylogeography of North American Odocoileus Deer based on mitochondrial DNA sequences.

43. Latch, E.K., Reding, D.M., Heffelfinger, J.R., Alcalá-Galván, C.H., and Rhodes, O.E. (2014). Range-wide Analysis of Genetic Structure in a Widespread, Highly Mobile Species (Odocoileus hemionus) Reveals the Importance of Historical Biogeography. Mol Ecol *23*, 3171–3190. 10.1111/mec.12803.

44. Cambronne, A. (2013). Deerland: America's Hunt for Ecological Balance and the Essence of Wildness.

45. Peres, T.M., and Altman, H. (2018). The Magic of Improbable Appendages: Deer Antler Objects in the Archaeological Record of the American South. Journal of Archaeological Science: Reports *20*, 888–895. 10.1016/j.jasrep.2017.10.028.

46. Adams, K.P., and Hamilton, R.J. (2011). Management History. In Biology and management of white-tailed deer, D. G. Hewitt, ed. (CRC Press).

47. Weitzel, E.M. (2021). Investigating overhunting of white-tailed deer (Odocoileus virginianus) in the late Holocene Middle Tennessee River Valley. Southeastern Archaeology *40*, 1–19. 10.1080/0734578X.2021.1873641.

48. Wolverton, S., Nagaoka, L., Densmore, J., and Fullerton, B. (2008). White-tailed deer harvest pressure & within-bone nutrient exploitation during the mid- to late Holocene in southeast Texas. Before Farming *2008*, 1–23. 10.3828/bfarm.2008.2.3.

49. McDonald, J.S., Miller, K.V., Association, Q.D.M., and Resources, D.B.W.S. of F. (2004). A History of White-tailed Deer Restocking in the United States, 1878 to 2004 (Quality Deer Management Assoc.).

50. Jensen, W.F., Bleich, V.C., and Whittaker, D.G. (2023). Historical Trends in Black-tailed Deer, Mule Deer, and Their Habitats. In Ecology and management of black-tailed and mule deer of North America, J. Heffelfinger, P. R. Krausman, and A. Cox, eds. (CRC Press).

51. Bergman, E.J., Doherty, P.F., White, G.C., and Holland, A.A. (2015). Density dependence in mule deer: a review of evidence. Wildlife Biology *21*, 18–29. 10.2981/wlb.00012.

52. Clements, D., and Young, A. (1997). A viewpoint: Rangeland health and mule deer habitat. JOURNAL OF RANGE MANAGEMENT.

53. Gill, R.B. (1999). Declining Mule Deer Populations in Colorado: Reasons and Responses (a report to the Colorado Legislature, November 1999) (Colorado Division of Wildlife).

54. Gruell, G.E. (1986). Post-1900 mule deer irruptions in the Intermountain West: Principal cause and influences (U.S. Department of Agriculture, Forest Service, Intermountain Research Station) 10.2737/INT-GTR-206.

55. Webb, G.K. (2018). Searching the internet to estimate deer population trends in the U.S., California, and Connecticut. IIS *19*, 163–173. 10.48009/2_iis_2018_163-173.

56. Deer Friendly Deer Population. Deer Friendly. https://www.deerfriendly.com/decline-of-deer-populations.

57. Andrews S. (2010). FastQC: a Quality Control Tool for High Throughput Sequence Data. Available online at: http://www.bioinformatics.babraham.ac.uk/projects/fastqc.

58. Bolger, A.M., Lohse, M., and Usadel, B. (2014). Trimmomatic: a flexible trimmer for Illumina sequence data. Bioinformatics *30*, 2114–2120. 10.1093/bioinformatics/btu170.

59. Li, H., and Durbin, R. (2009). Fast and Accurate Short Read Alignment with Burrows-Wheeler Transform. Bioinformatics *25*, 1754–1760. 10.1093/bioinformatics/btp324.

60. Li, H., Handsaker, B., Wysoker, A., Fennell, T., Ruan, J., Homer, N., Marth, G., Abecasis, G., Durbin, R., and 1000 Genome Project Data Processing Subgroup (2009). The Sequence Alignment/Map format and SAMtools. Bioinformatics *25*, 2078–2079. 10.1093/bioinformatics/btp352.

61. Broad Institute, GitHub Repository. (2019). “Picard Toolkit.” http://broadinstitute.github.io/picard/.

62. Tarasov, A., Vilella, A.J., Cuppen, E., Nijman, I.J., and Prins, P. (2015). Sambamba: fast processing of NGS alignment formats. Bioinformatics *31*, 2032–2034. 10.1093/bioinformatics/btv098.

63. McKenna, A., Hanna, M., Banks, E., Sivachenko, A., Cibulskis, K., Kernytsky, A., Garimella, K., Altshuler, D., Gabriel, S., Daly, M., et al. (2010). The Genome Analysis Toolkit: A MapReduce framework for analyzing next-generation DNA sequencing data. Genome Research *20*, 1297–1303. 10.1101/gr.107524.110.

64. Pedersen, B.S., and Quinlan, A.R. (2018). Mosdepth: Quick Coverage Calculation for Genomes and Exomes. Bioinformatics *34*, 867–868. 10.1093/bioinformatics/btx699.

65. Ewels, P., Magnusson, M., Lundin, S., and Käller, M. (2016). MultiQC: Summarize Analysis Results for Multiple Tools and Samples in a Single Report. Bioinformatics *32*, 3047–3048. 10.1093/bioinformatics/btw354.

66. Korneliussen, T.S., Albrechtsen, A., and Nielsen, R. (2014). ANGSD: Analysis of Next Generation Sequencing Data. BMC Bioinformatics *15*, 356. 10.1186/s12859-014-0356-4.

67. Meisner, J., and Albrechtsen, A. (2018). Inferring Population Structure and Admixture Proportions in Low-Depth NGS Data. Genetics *210*, 719–731. 10.1534/genetics.118.301336.

68. R Core Team (2021). R: A Language and Environment for Statistical Computing (R Foundation for Statistical Computing).

69. Skotte, L., Korneliussen, T.S., and Albrechtsen, A. (2013). Estimating Individual Admixture Proportions from Next Generation Sequencing Data. Genetics *195*, 693–702. 10.1534/genetics.113.154138.

70. Evanno, G., Regnaut, S., and Goudet, J. (2005). Detecting the Number of Clusters of Individuals Using the Software Structure: a Simulation Study. Mol Ecol *14*, 2611–2620. 10.1111/j.1365-294X.2005.02553.x.

71. Kopelman, N.M., Mayzel, J., Jakobsson, M., Rosenberg, N.A., and Mayrose, I. (2015). Clumpak: a Program for Identifying Clustering Modes and Packaging Population Structure Inferences Across K. Mol Ecol Resour *15*, 1179–1191. 10.1111/1755-0998.12387.

72. Martin, S. (2021). genomics_general. GitHub. https://github.com/simonhmartin/genomics_general.

73. Danecek, P., Auton, A., Abecasis, G., Albers, C.A., Banks, E., DePristo, M.A., Handsaker, R.E., Lunter, G., Marth, G.T., Sherry, S.T., et al. (2011). The variant call format and VCFtools. Bioinformatics *27*, 2156–2158. 10.1093/bioinformatics/btr330.

74. Chang, C.C., Chow, C.C., Tellier, L.C., Vattikuti, S., Purcell, S.M., and Lee, J.J. (2015). Second-generation PLINK: rising to the challenge of larger and richer datasets. GigaSci *4*, 7. 10.1186/s13742-015-0047-8.

633 75. Martin, M., Patterson, M., Garg, S., O Fischer, S., Pisanti, N., Klau, G.W., Schöenhuth, A., and
634 Marschall, T. (2016). WhatsHap: Fast and Accurate Read-based Phasing (Bioinformatics)
635 10.1101/085050.

636 76. Wang, K., Mathieson, I., O'Connell, J., and Schiffels, S. (2020). Tracking Human Population
637 Structure through Time from Whole Genome Sequences. PLoS Genet *16*, e1008552.
638 10.1371/journal.pgen.1008552.

639 77. Demarais, S., Miller, K.V., and Jacobson, H.A. (2000). White-tailed deer. In Ecology and
640 management of large mammals in North America, S. Demarais and P. R. Krausman, eds.
641 (Prentice Hall).

642 78. Deyoung, R.W., Demarais, S., Honeycutt, R.L., Rooney, A.P., Gonzales, R.A., and Gee, K.L.
643 (2003). Genetic Consequences of White-tailed Deer (Odocoileus virginianus) Restoration in
644 Mississippi. Molecular Ecology *12*, 3237–3252. 10.1046/j.1365-294X.2003.01996.x.

645 79. Gutenkunst, R.N., Hernandez, R.D., Williamson, S.H., and Bustamante, C.D. (2009). Inferring
646 the Joint Demographic History of Multiple Populations from Multidimensional SNP
647 Frequency Data. PLoS Genet *5*, e1000695. 10.1371/journal.pgen.1000695.

648 80. Portik, D.M., Leaché, A.D., Rivera, D., Barej, M.F., Burger, M., Hirschfeld, M., Rödel, M.,
649 Blackburn, D.C., and Fujita, M.K. (2017). Evaluating mechanisms of diversification in a
650 Guineo-Congolian tropical forest frog using demographic model selection. Mol Ecol *26*,
651 5245–5263. 10.1111/mec.14266.

652 81. Hijmans, R.J. (2022). raster: Geographic Data Analysis and Modeling.

653 82. Fick, S.E., and Hijmans, R.J. (2017). WorldClim 2: new 1-km spatial resolution climate
654 surfaces for global land areas. International Journal of Climatology *37*, 4302–4315.
655 10.1002/joc.5086.

656 83. Dormann, C.F., Elith, J., Bacher, S., Buchmann, C., Carl, G., Carré, G., Marquéz, J.R.G., Gruber,
657 B., Lafourcade, B., Leitão, P.J., et al. (2013). Collinearity: a review of methods to deal with it
658 and a simulation study evaluating their performance. Ecography *36*, 27–46. 10.1111/j.1600-
659 0587.2012.07348.x.

660 84. Oksanen, J., Simpson, G.L., Blanchet, F.G., Kindt, R., Legendre, P., Minchin, P.R., O'Hara,
661 R.B., Solymos, P., Stevens, M.H.H., Szoecs, E., et al. (2022). vegan: Community Ecology
662 Package.

663 85. O'Connell, J., Gurdasani, D., Delaneau, O., Pirastu, N., Ulivi, S., Cocca, M., Traglia, M., Huang,
664 J., Huffman, J.E., Rudan, I., et al. (2014). A General Approach for Haplotype Phasing across
665 the Full Spectrum of Relatedness. PLoS Genet *10*, e1004234.
666 10.1371/journal.pgen.1004234.

667 86. Garrison, E., Kronenberg, Z.N., Dawson, E.T., Pedersen, B.S., and Prins, P. (2022). A spectrum
668 of free software tools for processing the VCF variant call format: vcflib, bio-vcf, cyvcf2, hts-
669 nim and slivar. PLoS Comput Biol *18*, e1009123. 10.1371/journal.pcbi.1009123.

87. Grinberg, S. (2019). findPeaks. GitHub. https://github.com/stas-g/findPeaks/blob/master/find_peaks.R.

88. Pundir, S., Martin, M.J., O'Donovan, C., and The UniProt Consortium (2016). UniProt Tools. Current Protocols in Bioinformatics *53*. 10.1002/0471250953.bi0129s53.

89. Skoglund, P., and Reich, D. (2016). A genomic view of the peopling of the Americas. Current Opinion in Genetics & Development *41*, 27–35. 10.1016/j.gde.2016.06.016.

90. Smith, B.T., Gehara, M., and Harvey, M.G. (2021). The demography of extinction in eastern North American birds. Proc. R. Soc. B. *288*, 20201945. 10.1098/rspb.2020.1945.

91. Ito, T., Hayakawa, T., Suzuki–Hashido, N., Hamada, Y., Kurihara, Y., Hanya, G., Kaneko, A., Natsume, T., Aisu, S., Honda, T., et al. (2021). Phylogeographic History of Japanese Macaques. J Biogeogr, jbi.14087. 10.1111/jbi.14087.

92. Colella, J.P., Lan, T., Talbot, S.L., Lindqvist, C., and Cook, J.A. (2021). Whole-genome Resequencing Reveals Persistence of Forest-Associated Mammals in Late Pleistocene Refugia along North America's North Pacific Coast. J. Biogeogr. *48*, 1153–1169. 10.1111/jbi.14068.

93. Baca, M. (2020). Diverse responses of common vole (Microtus arvalis) populations to Late Glacial and Early Holocene climate changes - Evidence from ancient DNA. Quaternary Science Reviews, 13.

94. Meiri, M., Lister, A., Kosintsev, P., Zazula, G., and Barnes, I. (2020). Population dynamics and range shifts of moose (Alces alces) during the Late Quaternary. J Biogeogr *47*, 2223–2234. 10.1111/jbi.13935.

95. Dussex, N., Alberti, F., Heino, M.T., Olsen, R.-A., van der Valk, T., Ryman, N., Laikre, L., Ahlgren, H., Askeyev, I.V., Askeyev, O.V., et al. (2020). Moose Genomes Reveal Past Glacial Demography and the Origin of Modern Lineages. BMC Genomics *21*, 854. 10.1186/s12864-020-07208-3.

96. Ersmark, E., Baryshnikov, G., Higham, T., Argant, A., Castaños, P., Döppes, D., Gasparik, M., Germonpré, M., Lidén, K., Lipecki, G., et al. (2019). Genetic turnovers and northern survival during the last glacial maximum in European brown bears. Ecol Evol *9*, 5891–5905. 10.1002/ece3.5172.

97. Loog, L., Thalmann, O., Sinding, M.S., Schuenemann, V.J., Perri, A., Germonpré, M., Bocherens, H., Witt, K.E., Samaniego Castruita, J.A., Velasco, M.S., et al. (2020). Ancient DNA suggests modern wolves trace their origin to a Late Pleistocene expansion from Beringia. Mol Ecol *29*, 1596–1610. 10.1111/mec.15329.

98. Combe, F.J., Jaster, L., Ricketts, A., Haukos, D., and Hope, A.G. (2021). Population Genomics of Free-ranging Great Plains White-tailed and Mule deer Reflects a Long History of Inter-specific Hybridization. Evolutionary Applications *15*, 111–132. 10.1111/eva.13330.

99. Moscarella, R.A., Aguilera, M., and Escalante, A.A. (2003). Phylogeography, Population Structure, and Implications for Conservation of White-tailed Deer (Odocoileus Virginianus) in Venezuela. Journal of Mammalogy *84*, 1300–1315. 10.1644/BRB-028.

100. Villanova, V.L., Hughes, P.T., and Hoffman, E.A. (2017). Combining genetic structure and demographic analyses to estimate persistence in endangered Key deer (Odocoileus virginianus clavium). Conserv Genet *18*, 1061–1076. 10.1007/s10592-017-0958-2.

101. Cars, B., Kessler, C., Hoffman, E.A., Côté, S.D., Koelsch, D., and Shafer, A.B.A. (2023). Island demographics and trait associations in white-tailed deer.

102. U.S. Fish & Wildlife Service (1967). Endangered Species List.

103. Forrester, T.D., and Wittmer, H.U. (2013). A review of the population dynamics of mule deer and black-tailed deer Odocoileus hemionus in North America: Population dynamics of mule deer and black-tailed deer. Mammal Review *43*, 292–308. 10.1111/mam.12002.

104. Peart, C.R., Tusso, S., Pophaly, S.D., Botero-Castro, F., Wu, C.-C., Aurioles-Gamboa, D., Baird, A.B., Bickham, J.W., Forcada, J., Galimberti, F., et al. (2020). Determinants of genetic variation across eco-evolutionary scales in pinnipeds. Nat Ecol Evol *4*, 1095–1104. 10.1038/s41559-020-1215-5.

105. Mautz, W., Pekins, P., and Warren, J. (1985). Cold temperature effects on metabolic rate of white-tailed, mule, and black-tailed deer in winter coat. Biology of deer production. Bulletin *22*, 453–457.

106. Lynch, V.J., Bedoya-Reina, O.C., Ratan, A., Sulak, M., Drautz-Moses, D.I., Perry, G.H., Miller, W., and Schuster, S.C. (2015). Elephantid Genomes Reveal the Molecular Bases of Woolly Mammoth Adaptations to the Arctic. Cell Reports *12*, 217–228. 10.1016/j.celrep.2015.06.027.

107. Budd, K., Berkman, L.K., Anderson, M., Koppelman, J., and Eggert, L.S. (2018). Genetic Structure and Recovery of White-tailed Deer in Missouri. Jour. Wild. Mgmt. *82*, 1598–1607. 10.1002/jwmg.21546.

108. Fuller, J., Ferchaud, A., Laporte, M., Le Luyer, J., Davis, T.B., Côté, S.D., and Bernatchez, L. (2020). Absence of founder effect and evidence for adaptive divergence in a recently introduced insular population of white-tailed deer (Odocoileus virginianus). Mol Ecol *29*, 86–104. 10.1111/mec.15317.

109. Nelson, S.L., Taylor, S.A., and Reuter, J.D. (2021). An isolated white-tailed deer (Odocoileus virginianus) population on St. John, US Virgin Islands shows low inbreeding and comparable heterozygosity to other larger populations. Ecol Evol *11*, 2775–2781. 10.1002/ece3.7230.

110. Wootton, E., Robert, C., Taillon, J., Côté, S.D., and Shafer, A.B.A. (2023). Genomic health is dependent on long-term population demographic history. Molecular Ecology *32*, 1943–1954. 10.1111/mec.16863.

111. Campbell, T.A., and VerCauteren, K.C. (2011). Diseases and Parasites. In Biology and management of white-tailed deer (CRC Press), pp. 220–240.

112. Russell, T., Cullingham, C., Ball, M., Pybus, M., and Coltman, D. (2021). Extent and direction of introgressive hybridization of mule and white-tailed deer in western Canada. Evol Appl *14*, 1914–1925. 10.1111/eva.13250.

113. Shawlot, W., Vazquez-Chantada, M., Wallingford, J.B., and Finnell, R.H. (2015). Rfx2 is required for spermatogenesis in the mouse: Rfx2 mouse knockout. genesis *53*, 604–611. 10.1002/dvg.22880.

114. Maddirevula, S., Coskun, S., Al-Qahtani, M., Aboyousef, O., Alhassan, S., Aldeery, M., and Alkuraya, F.S. (2022). ASTL is mutated in female infertility. Hum Genet *141*, 49–54. 10.1007/s00439-021-02388-8.

115. Ding, X., Fragoza, R., Singh, P., Zhang, S., Yu, H., and Schimenti, J.C. (2020). Variants in RABL2A causing male infertility and ciliopathy. Human Molecular Genetics *29*, 3402–3411. 10.1093/hmg/ddaa230.

116. DeVivo, M.T., Edmunds, D.R., Kauffman, M.J., Schumaker, B.A., Binfet, J., Kreeger, T.J., Richards, B.J., Schätzl, H.M., and Cornish, T.E. (2017). Endemic chronic wasting disease causes mule deer population decline in Wyoming. PLoS ONE *12*, e0186512. 10.1371/journal.pone.0186512.

117. Seabury, C.M., Oldeschulte, D.L., Bhattarai, E.K., Legare, D., Ferro, P.J., Metz, R.P., Johnson, C.D., Lockwood, M.A., and Nichols, T.A. (2020). Accurate Genomic Predictions for Chronic Wasting Disease in U.S. White-Tailed Deer. G3 Genes|Genomes|Genetics *10*, 1433–1441. 10.1534/g3.119.401002.

118. Frankham, R. (1995). Effective population size/adult population size ratios in wildlife: a review. Genet. Res. *66*, 95–107. 10.1017/S0016672300034455.

119. Ferchaud, A.-L., Perrier, C., April, J., Hernandez, C., Dionne, M., and Bernatchez, L. (2016). Making sense of the relationships between Ne, Nb and Nc towards defining conservation thresholds in Atlantic salmon (Salmo salar). Heredity *117*, 268–278. 10.1038/hdy.2016.62.

120. Waples, R.S., Luikart, G., Faulkner, J.R., and Tallmon, D.A. (2013). Simple life-history traits explain key effective population size ratios across diverse taxa. Proc. R. Soc. B. *280*, 20131339. 10.1098/rspb.2013.1339.

121. Dedato, M.N., Robert, C., Taillon, J., Shafer, A.B.A., and Côté, S.D. (2022). Demographic history and conservation genomics of caribou (Rangifer tarandus) in Québec. Evolutionary Applications *15*, 2043–2053. 10.1111/eva.13495.

Tables

Table 1: Tajima's D, nucleotide diversity and F_{ROH} for our four populations, F_{ROH} as percentage of the N90 scaffolds.

	Tajima's D	Nucleotide diversity (π)	F_{ROH}
WTD_{ML}	-0.89	0.0068	0.89 %
WTD_{KEY}	0.11	0.0038	1.38 %
MD_{MD}	-0.29	0.0036	0.30 %
MD_{BTD}	-0.13	0.0037	0.28 %

Table 2: Best model parameter values from δaδi per comparison and corresponding 95% CI computed on 100 bootstraps.

		nu				m			T				
	Theta	nu1	nu2	nu3	nuA	m1	m2	mA	T1	T1a	T1b	T2	T3
WTD_{KEY} & WTD_{ML} & MD													
Parameters	21'150.17	0.56	1.73	0.20	4.02	0.86	2.15	-	0.57	-	-	0.12	0.02
2.5% CI		0.44	1.34	0.18	0.06	0.07	0.11	-	0.03	-	-	0.02	0.06
97.5% CI		2.61	7.47	2.04	24.23	0.49	2.70	-	3.27	-	-	3.95	4.10
WTD_{ML} & MD_{BTD} & MD_{MD}													
Parameters	20'887.17	2.09	0.29	0.27	0.84	0.79	0.79	0.02	-	0.11	0.86	0.04	-
2.5% CI		1.17	0.13	0.10	0.07	0.04	0.10	0.03	-	0.04	0.05	0.02	-
97.5% CI		10.03	5.15	9.23	12.95	0.62	12.91	17.37	-	5.07	14.09	8.98	-

Table 3: Anova of the RDA for full and conditional models as well as number of outlier SNPs for each predictor in the full model. Significant p-values are highlighted in bold.

		Adjusted R^2	*bio1*	*bio2*	*bio8*	*bio12*	*bio14*	*bio15*	*bio16*	*bio18*	*Longitude*	*Species*
Interspecies												
~ BIOs + Long + SP	P-value	16.55%	0.004	0.001	0.012	0.009	-	0.001	-	-	0.001	0.001
	Variance explained		2.58%	3.12%	1.95%	1.95%	-	3.54%	-	-	3.55%	7.96%
	number of outlier SNPs		5448	768	760	2491		47			2820	2101
MD												
~ BIOs + Long	P-value	8.82%	0.093	0.001	-	-	0.116	0.355	0.012	0.374	0.219	-
	Variance explained		5.67%	9.82%	-	-	5.48%	4.82%	6.72%	4.83%	5.04%	-
	number of outlier SNPs		99	540	-	-	690	1	4452	0	1652	-
~ BIOs + Condition(Long)	P-value	4.11%	0.119	0.032	-	-	0.167	0.336	0.003	0.476	-	-
	Variance explained		5.96%	6.23%	-	-	5.84%	5.53%	7.29%	5.35%	-	-
~ Condition(BIOs) + Long	P-value	0.35%	-	-	-	-	-	-	-	-	0.445	-
	Variance explained		-	-	-	-	-	-	-	-	8.05%	-
WTD												
~ BIOs + Long	P-value	6.32%	0.001	0.001	0.034	-	-	0.001	-	-	0.001	-
	Variance explained		3.37%	3.89%	2.11%	-	-	2.99%	-	-	2.96%	-
	number of outlier SNPs		5625	4487	1025	-	-	209	-	-	777	-
~ BIOs + Condition(Long)	P-value	4.64%	0.001	0.001	0.038	-	-	0.001	-	-	-	-
	Variance explained		3.50%	3.57%	2.18%	-	-	2.94%	-	-	-	-
~ Condition(BIOs) + Long	P-value	1.26%	-	-	-	-	-	-	-	-	0.001	-
	Variance explained		-	-	-	-	-	-	-	-	3.38%	-

Figures

A

B

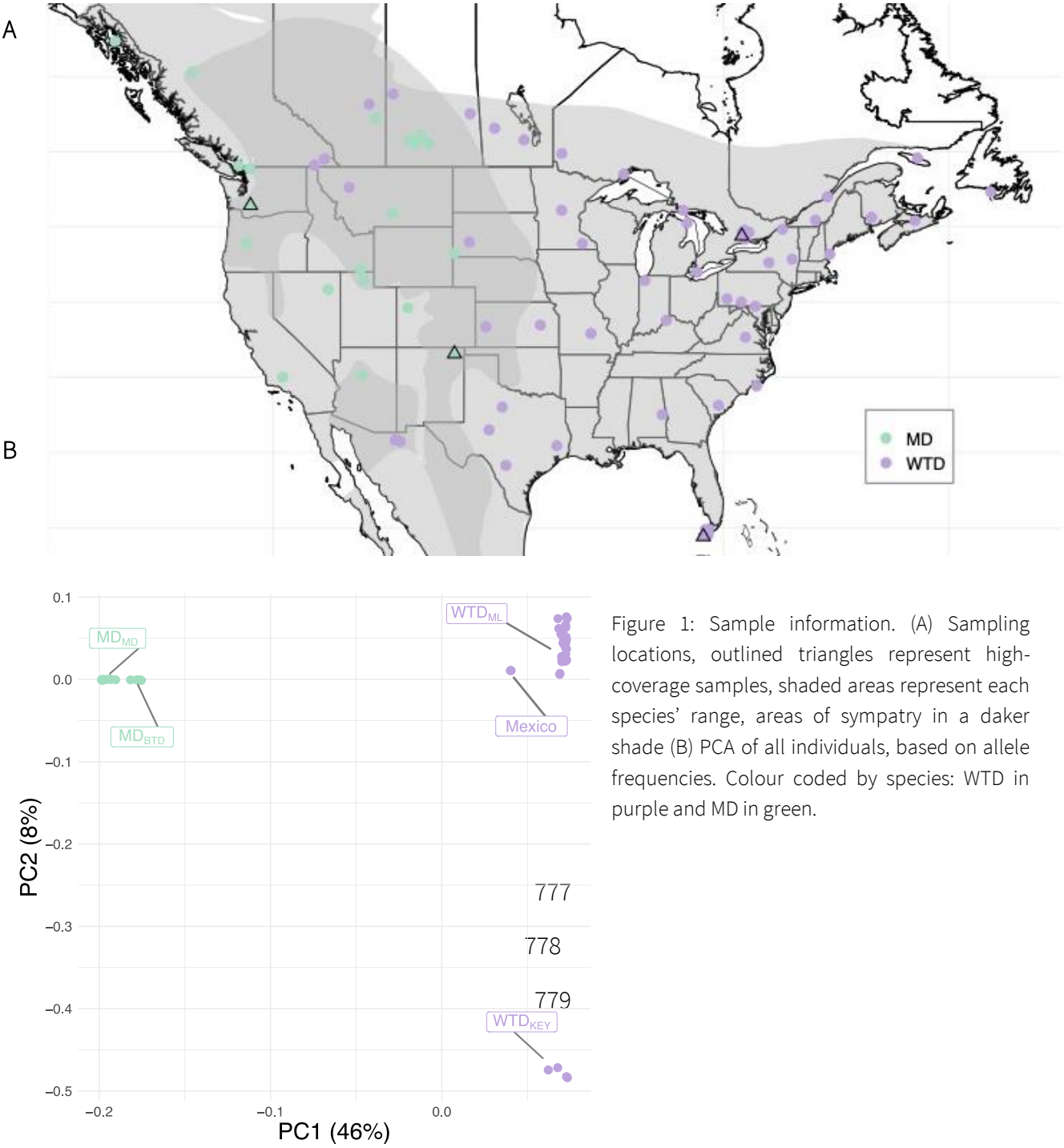

Figure 1: Sample information. (A) Sampling locations, outlined triangles represent high-coverage samples, shaded areas represent each species' range, areas of sympatry in a daker shade (B) PCA of all individuals, based on allele frequencies. Colour coded by species: WTD in purple and MD in green.

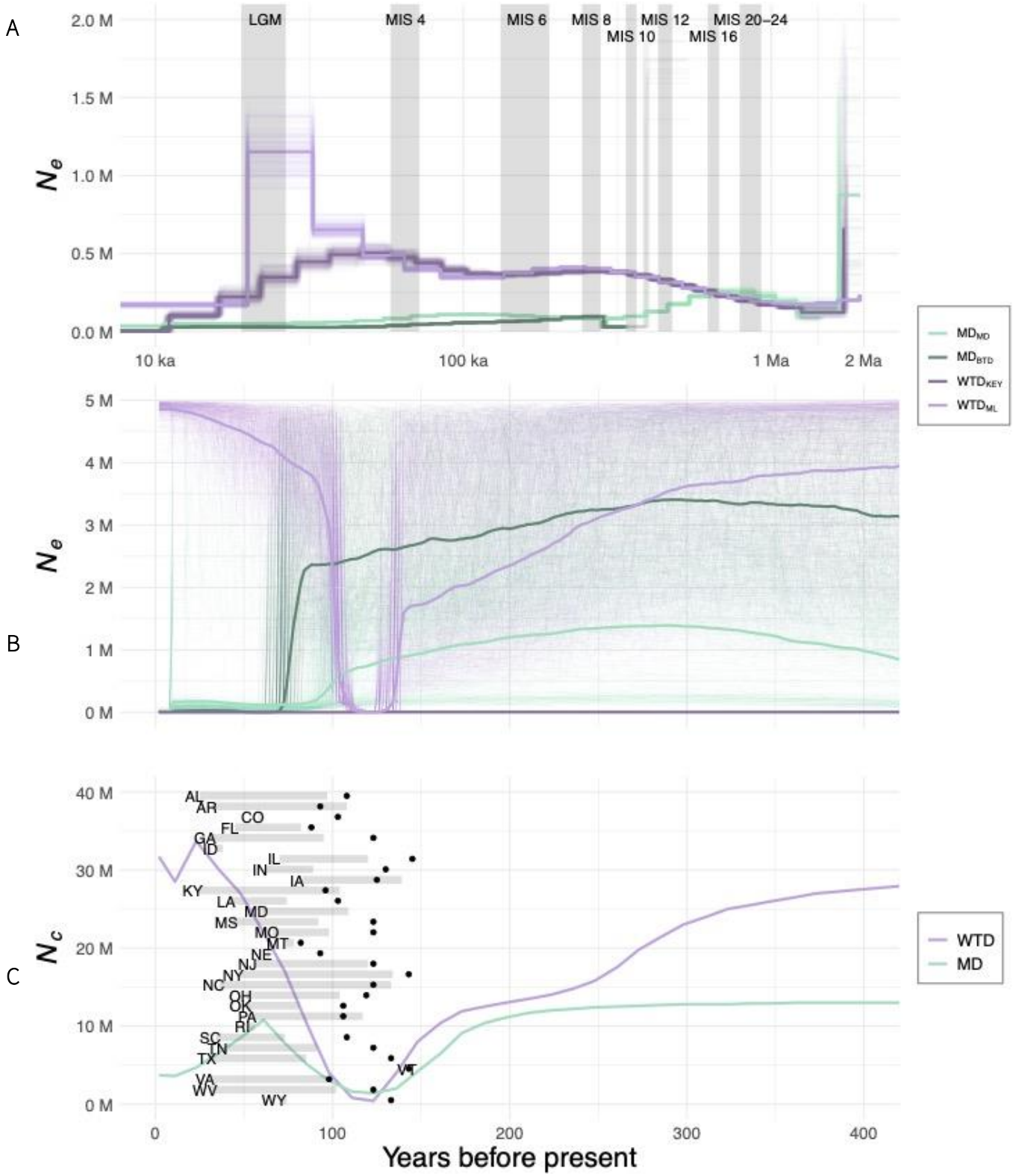

Figure 2: Demographic inference. (A) Changes in population size of four high coverage samples as estimated by MSMC2, x-axis represent years before present, shaded areas symbolise full glacial periods (Batchelor et al., 2019). (B) Recent changes in N_e computed by GONE on all samples with bootstraps. (C) Estimated WTD & MD population in the US from Webb (2018) with WTD restocking period for 30 US states (grey rectangles) and corresponding state's year with lowest WTD population (black points) from McDonald et al. (2004).

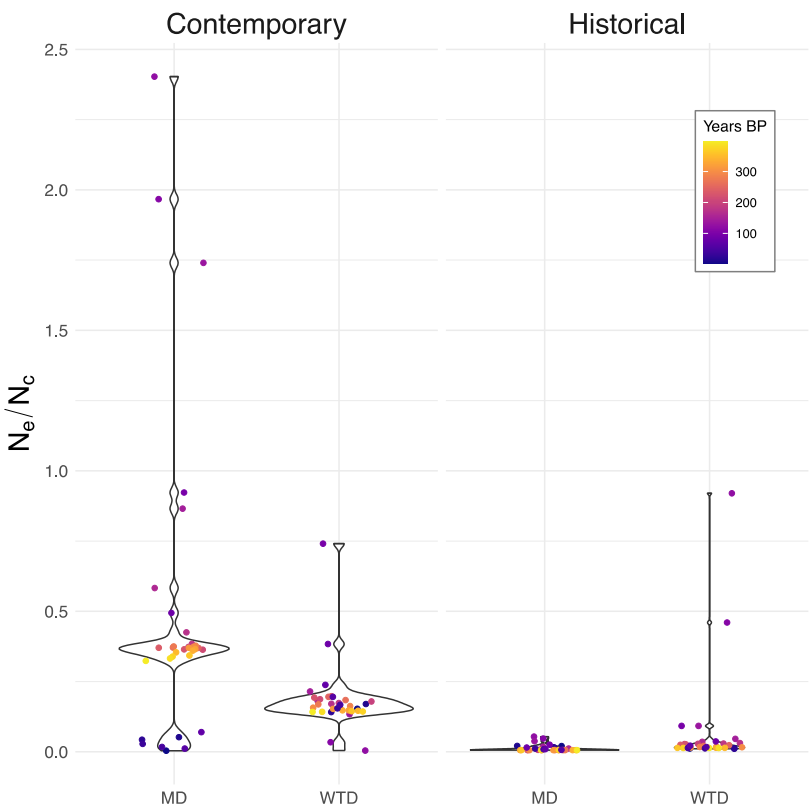

Figure 3: Contemporary and historical N_e/N_c ratio over time, point colour indicates time before present, N_e of the historical ratio taken from NuA values in the δaδi analysis.

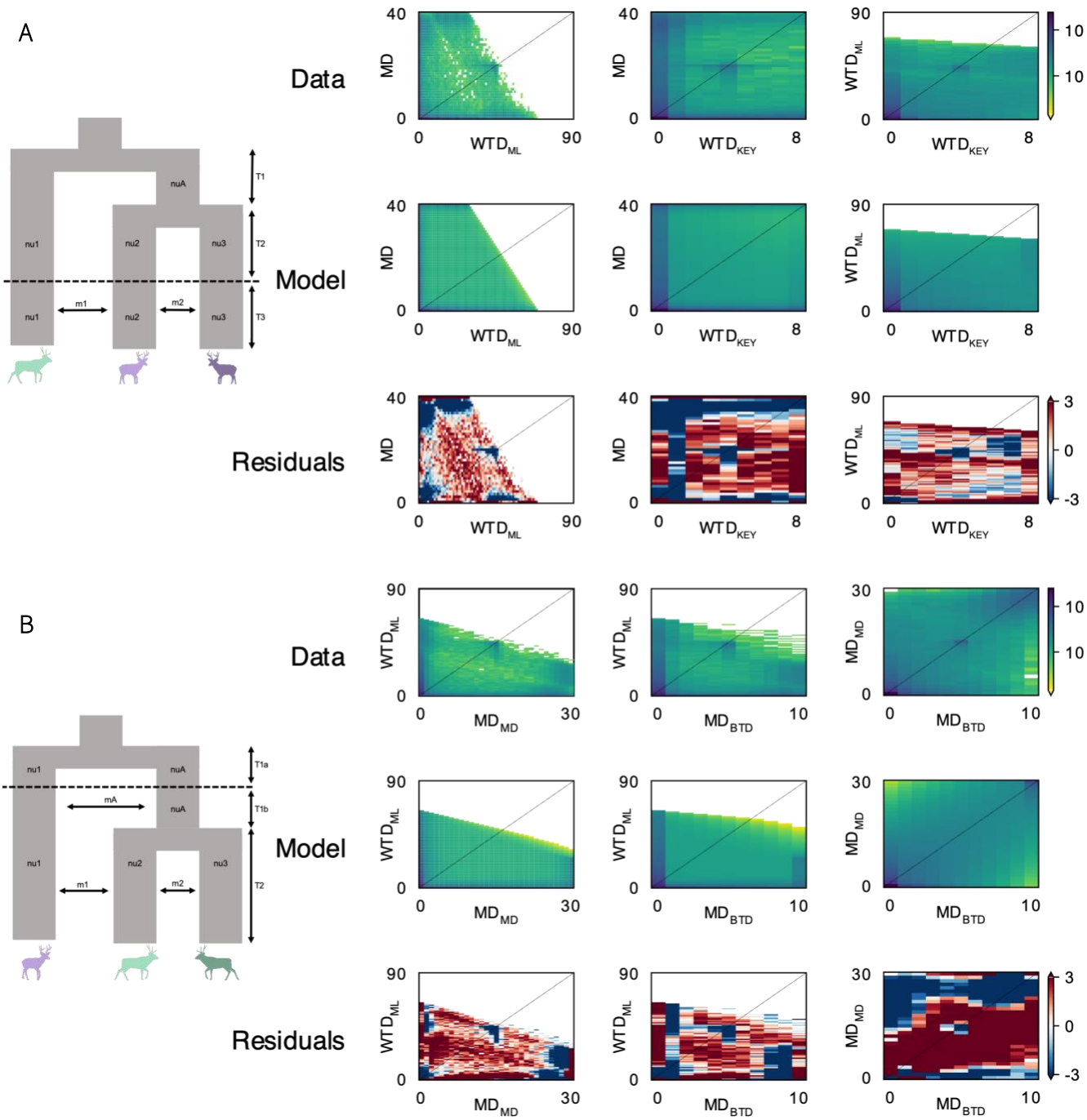

Figure 4: Three populations models in δaδI with best model schema on the right and 2D spectra on the right. (A) MD – WTD_{ML} – WTD_{KEY} comparisons, with MD in green, WTD_{ML} in light and WTD_{KEY} in dark purple. (B) WTD_{ML} – MD_{MD} – MD_{BTD} comparison with WTD_{ML} in light purple, MD_{MD} in light green and MD_{BTD} in dark green.